



Study of astrophysical perpendicular shocks for intermediate Mach numbers



Valentine Devos, Dr. Artem Bohdan, Dr. Frank Jenko

Contents

- Main objective
- Shock structure and instabilities
- Theoretical expectations
- PIC simulations and setup
- First simulations and results
- Future steps

Main Objective

→ Study of perpendicular collisionless shock and electron acceleration processes

Earth's bow shock and magnetosphere



Whistler Instability

Credit: ESA/AOES Medialab

Supernovae remnants



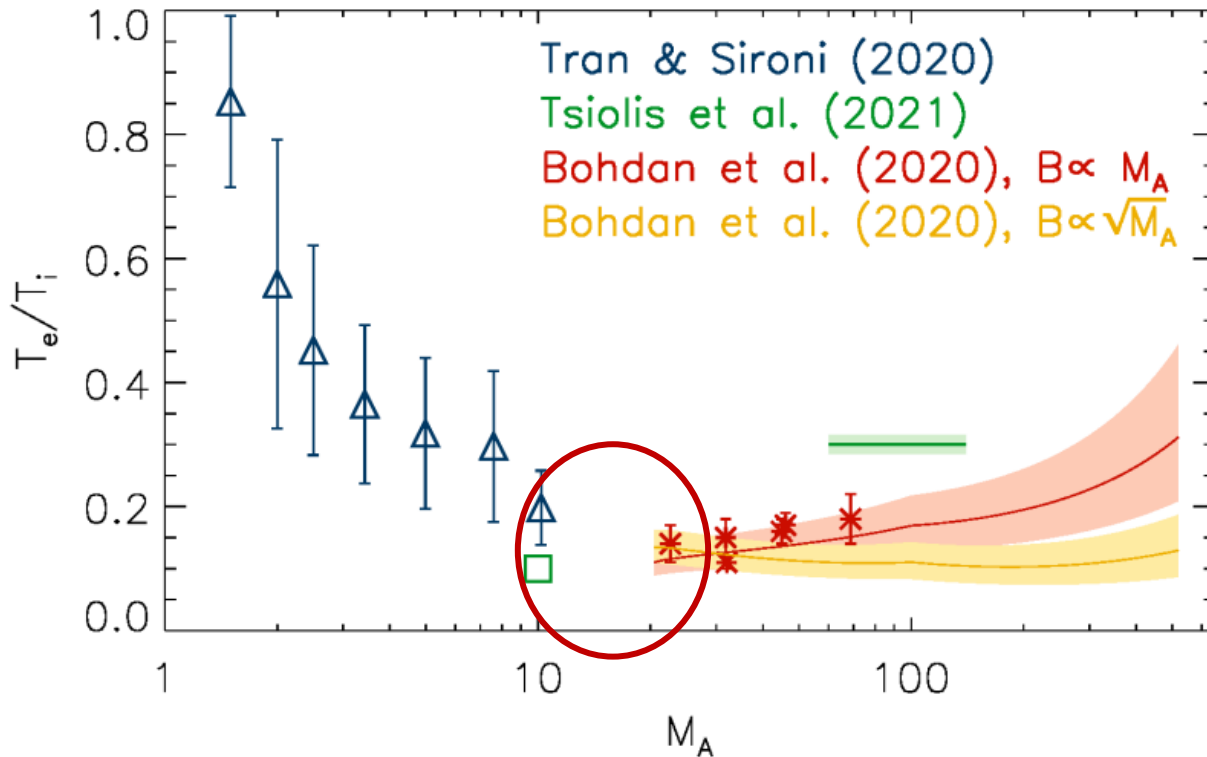
Weibel Instability

Credit: NASA, ESA, CSA, STSCI

M_A

Main Objective

→ Study of perpendicular collisionless shock and electron acceleration processes

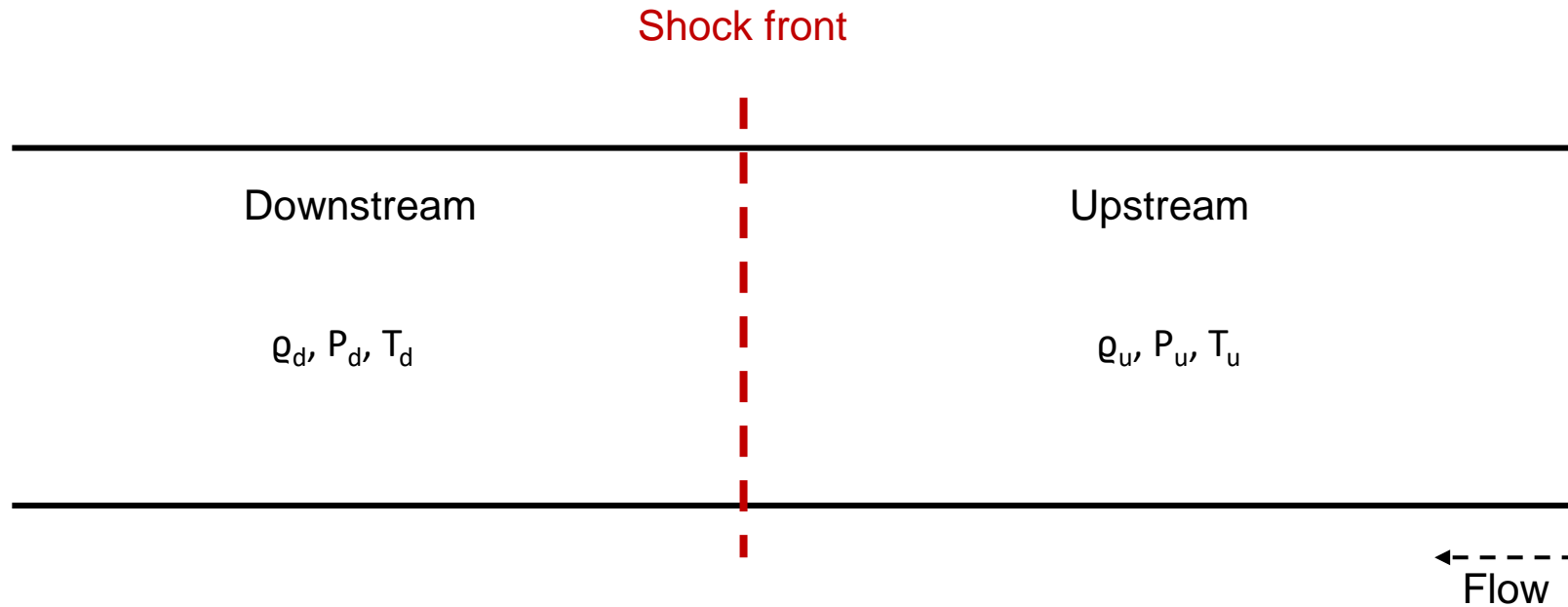


→ Depending on M_A , different kind of instabilities can arise

Intermediate Mach numbers

- Transition between Whistler and Weibel instabilities
- How does it affect electron heating and acceleration processes ?

Shock structure

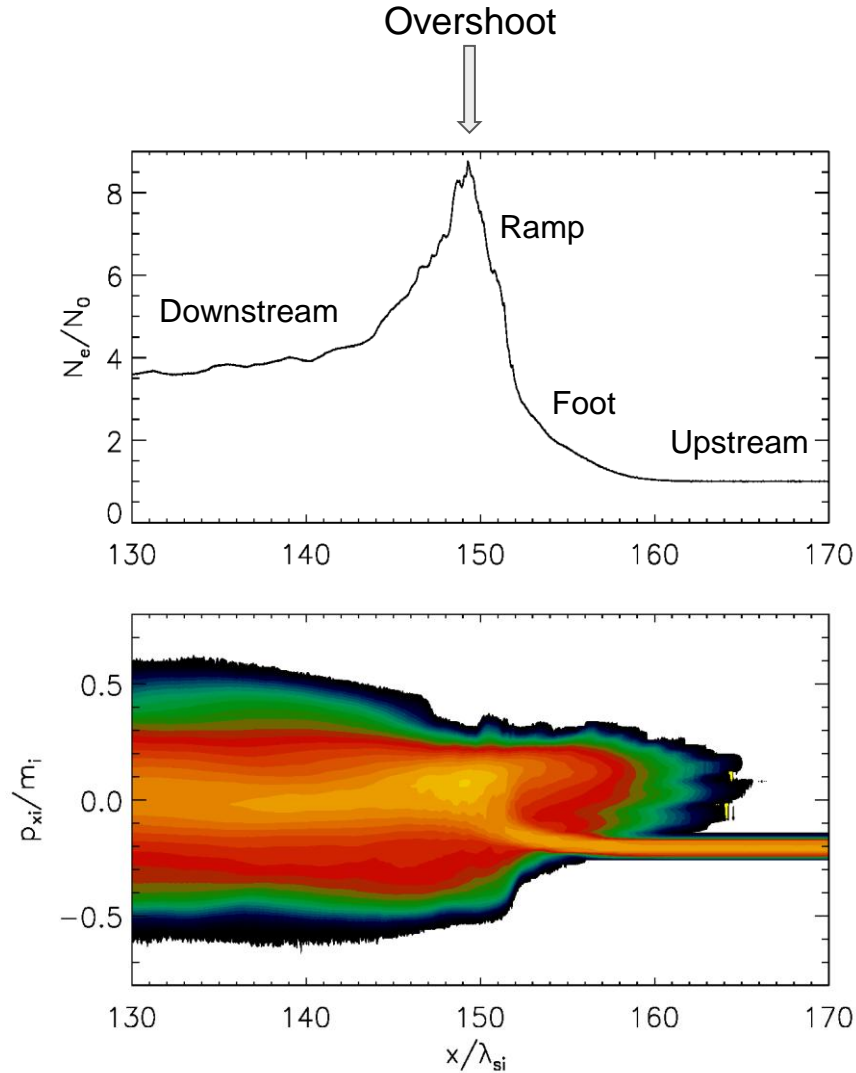


Sonic Mach number: $M_s = \frac{u}{a} = \left(\frac{\rho u^2}{\gamma P} \right)^{1/2}$

Alfvénic Mach number: $M_A = \frac{u}{u_A} = \left(\frac{\mu_0 \rho u^2}{B} \right)^{1/2}$

Shock structure

Perpendicular shock → Magnetic field perpendicular to the shock normal



Weibel and Whistler instabilities;

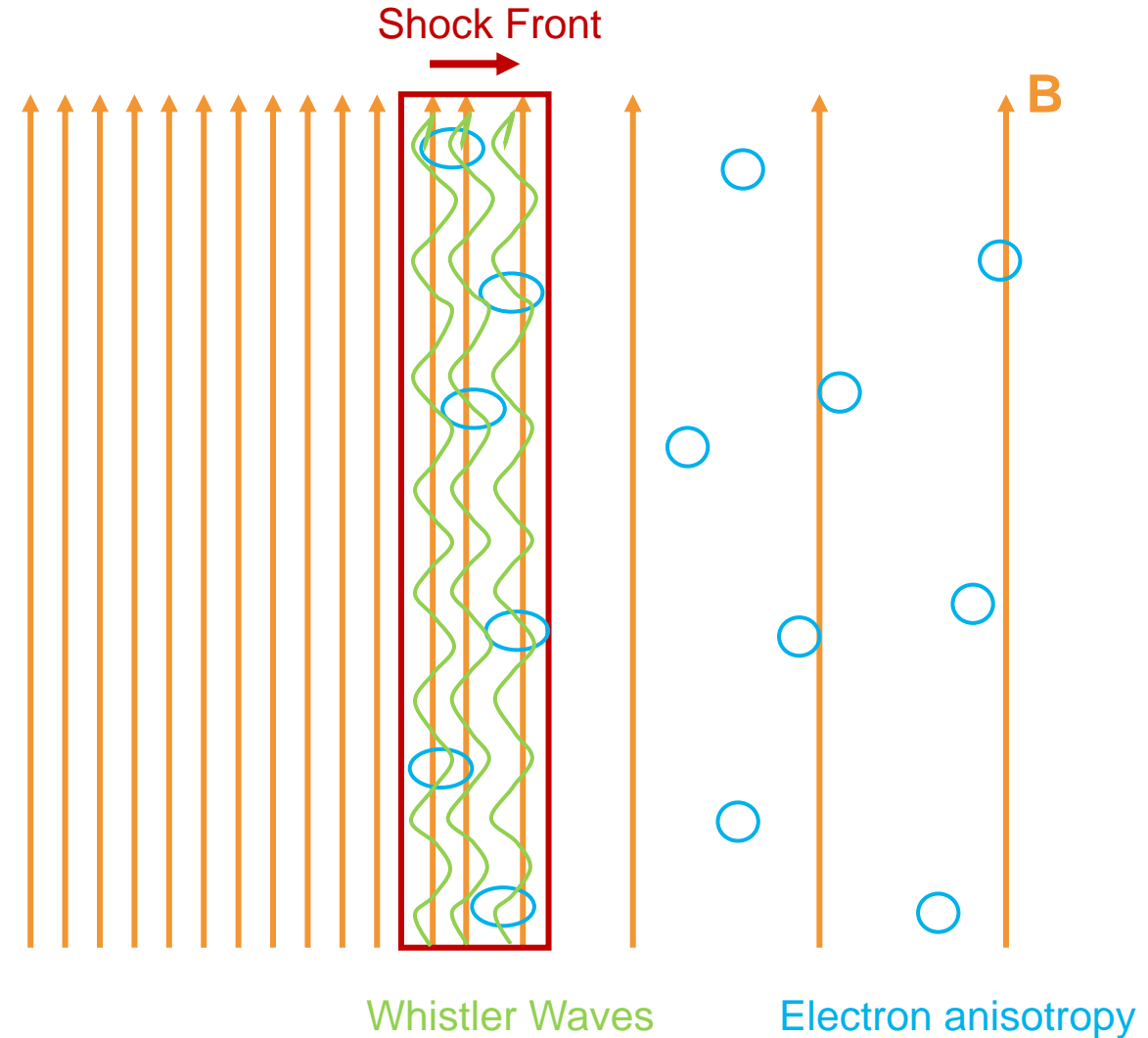
- Driven by 2-streams, depending on the Mach number
- Can be treated both like T° anisotropies or 2-beams.

Instabilities – Whistler anisotropy instability

Whistler Instability

$$M_A < 10$$

- Occurs in magnetized plasmas due to anisotropy in the particle distribution
- Generates Whistler waves, with typical frequency around the electron cyclotron frequency Ω_e , that propagates along the **B** lines
- Wave-particle interaction: acceleration and heating particles in the plasma
- If M_A is too high, the interaction between the whistler wave and the electrons will be weakened so that the instability's growth rate decreases. The Mach number influences how steep the shock ramp is and, in turn, the anisotropy or beams driving the instability

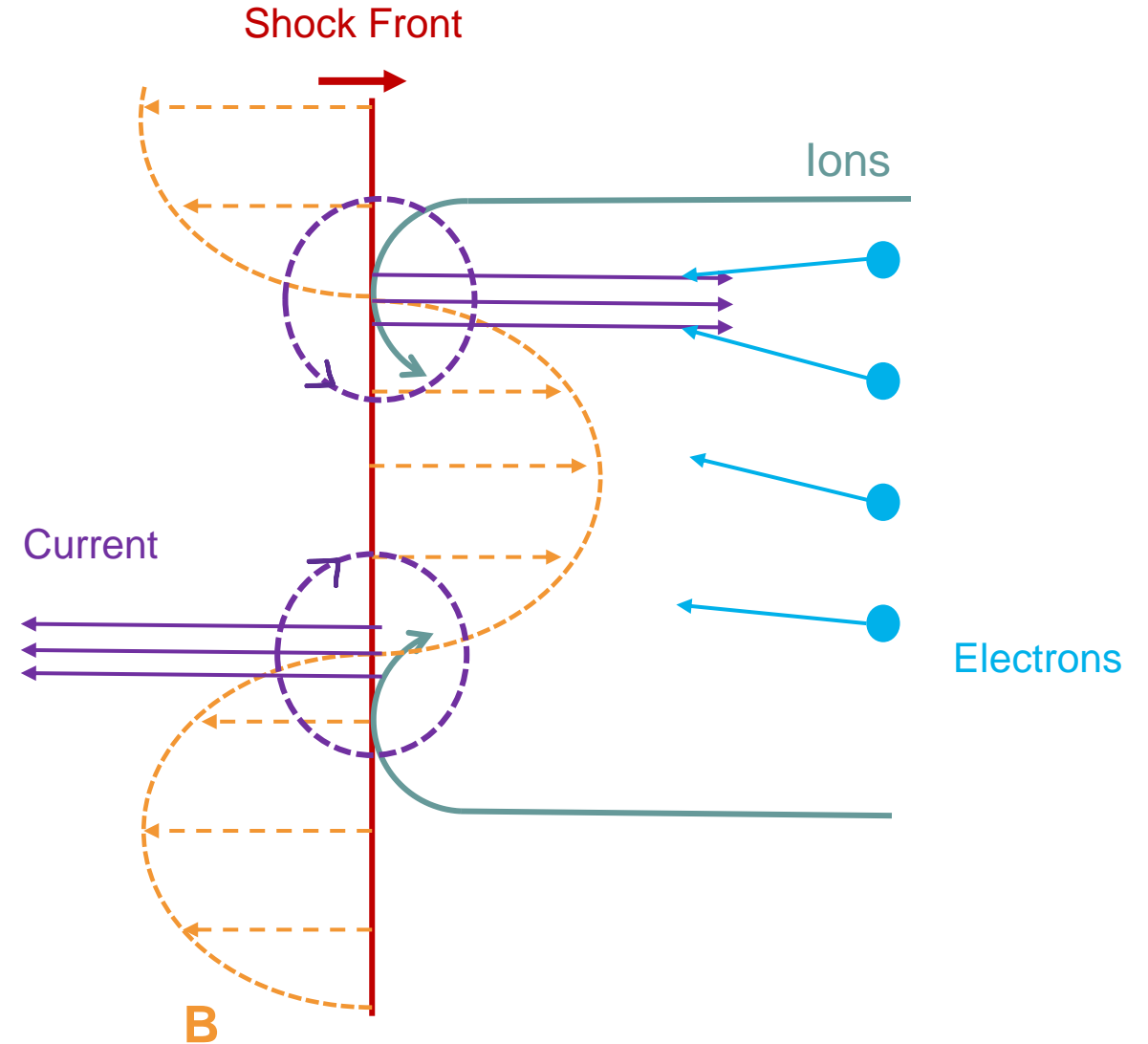


Instabilities – Weibel 2-stream instability

Weibel Instability

$$M_A > 25$$

- Occurs in magnetized plasmas due to anisotropy in the particle distribution + counter-streaming particles population
- The shock induces ions to move at different velocities \rightarrow creation of currents \mathbf{J} . By Ampère's law, \mathbf{J} creates \mathbf{B} . Feedback loop; \mathbf{B} couple back to the motion of particles such that the instability grows. Establishment of current filaments.
- Wave-particle interaction: acceleration and heating particles in the plasma
- Need a sufficient domination of the flow motion compare to the magnetic forces (i.e. high M_A). Higher Mach numbers can enhance ion reflection and increase the free energy available for the instability



Whistler Condition

Condition on the electron temperature anisotropy

$$\frac{T_{e\perp}}{T_{e\parallel}} - 1 \approx \frac{0.21}{\beta_{e\parallel}^{0.6}}$$

- $T_{e\perp}$ and $T_{e\parallel}$ are respectively the perpendicular and parallel temperature of electrons
- With $\xi \approx 1/3$, Γ the growth rate, and ω_{pi} the ion plasma frequency
- $\beta_{e\parallel}$ is the beta of electrons parallel to the magnetic field

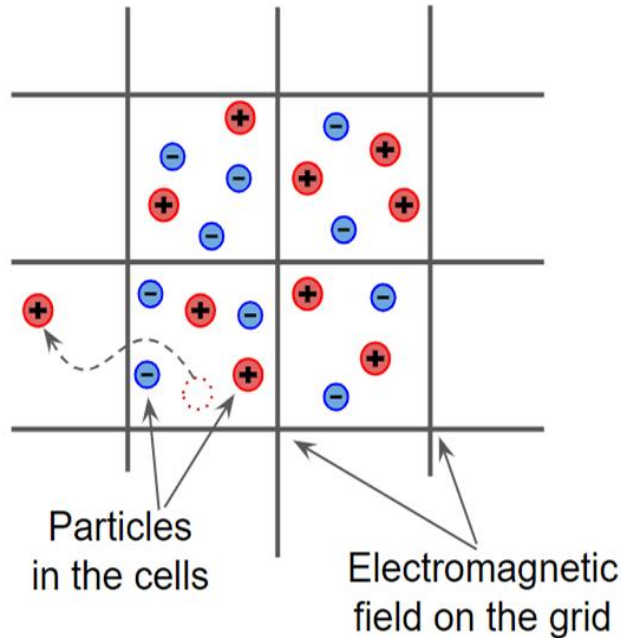
Weibel Condition

Needs a sufficient number of exponential growth cycles:

$$N_w = M_A \frac{c}{v_{sh}} \frac{\Gamma}{\omega_{pi}} \xi,$$

- c = light speed, v_{sh} = shock velocity
- With $\xi \approx 1/3$, Γ the growth rate, and ω_{pi} the ion plasma frequency
- In our case, $N_w \propto M_A/6$

PIC simulation



- Vlasov equation

$$\frac{\partial f_l}{\partial t} + \mathbf{v} \cdot \frac{\partial f_l}{\partial \mathbf{x}} + q_l [\mathbf{E}(\mathbf{x}, t) + \frac{1}{c} \mathbf{v} \times \mathbf{B}(\mathbf{x}, t)] \cdot \frac{\partial f_l}{\partial \mathbf{p}} = 0$$

- Lorentz force

$$\mathbf{F} = q(\mathbf{E} + \frac{1}{c} \mathbf{v} \times \mathbf{B})$$

- Maxwell equations

$$\nabla \cdot \mathbf{E} = 4\pi\rho, \nabla \cdot \mathbf{B} = 0, \nabla \times \mathbf{E} = -\frac{1}{c} \frac{\partial \mathbf{B}}{\partial t}, \nabla \times \mathbf{B} = \frac{1}{c} \frac{\partial \mathbf{E}}{\partial t} + \frac{4\pi}{c} \mathbf{j}$$

→ **THATMPI code** (Two-and-a-Half-Dimensional Advanced Stanford code with Message Passing Interface).

This code is a 2D3V-adapted and modified version of the relativistic electromagnetic PIC code TRISTAN (Three-Dimensional Stanford) [1] with Message Passing Interface-based (MPI) parallelization [2]

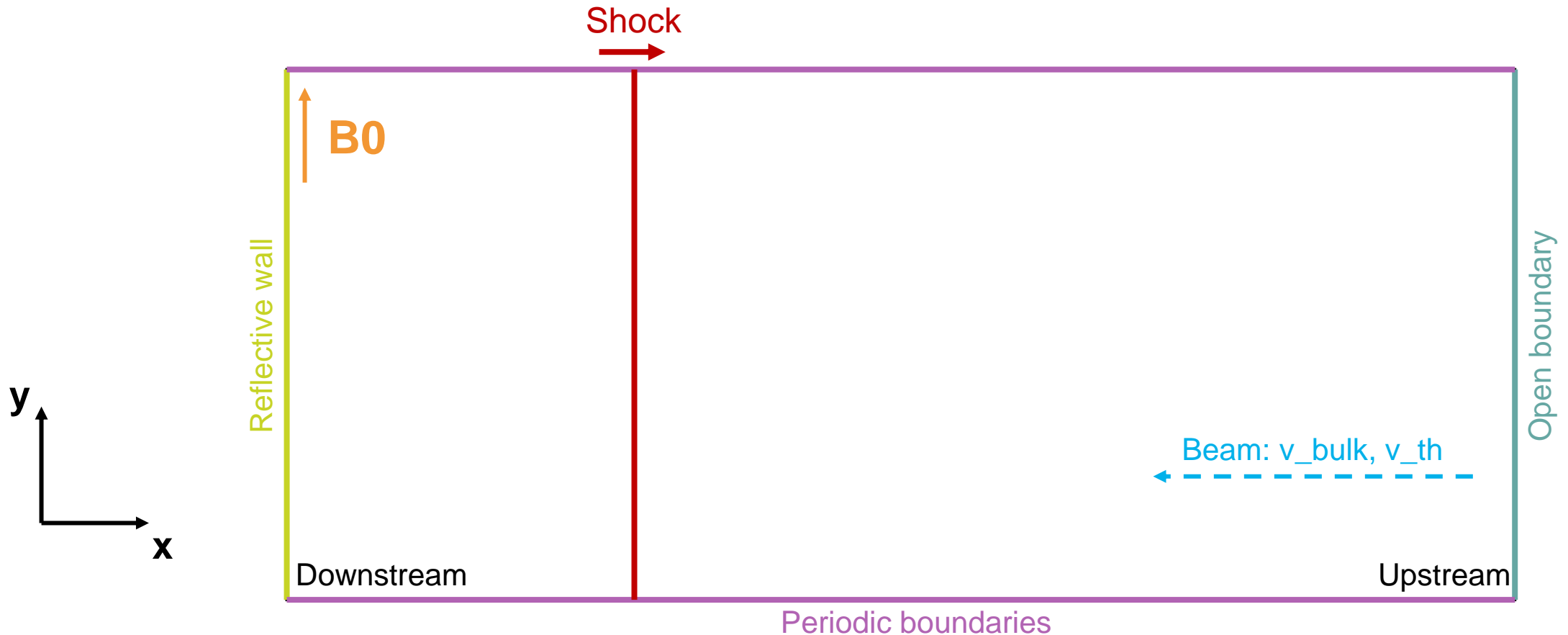
[1] Buneman, 1993

[2] Niemiec et al., 2008

PIC simulation - setup

Injection method; box with a reflective wall and a plasma beam.

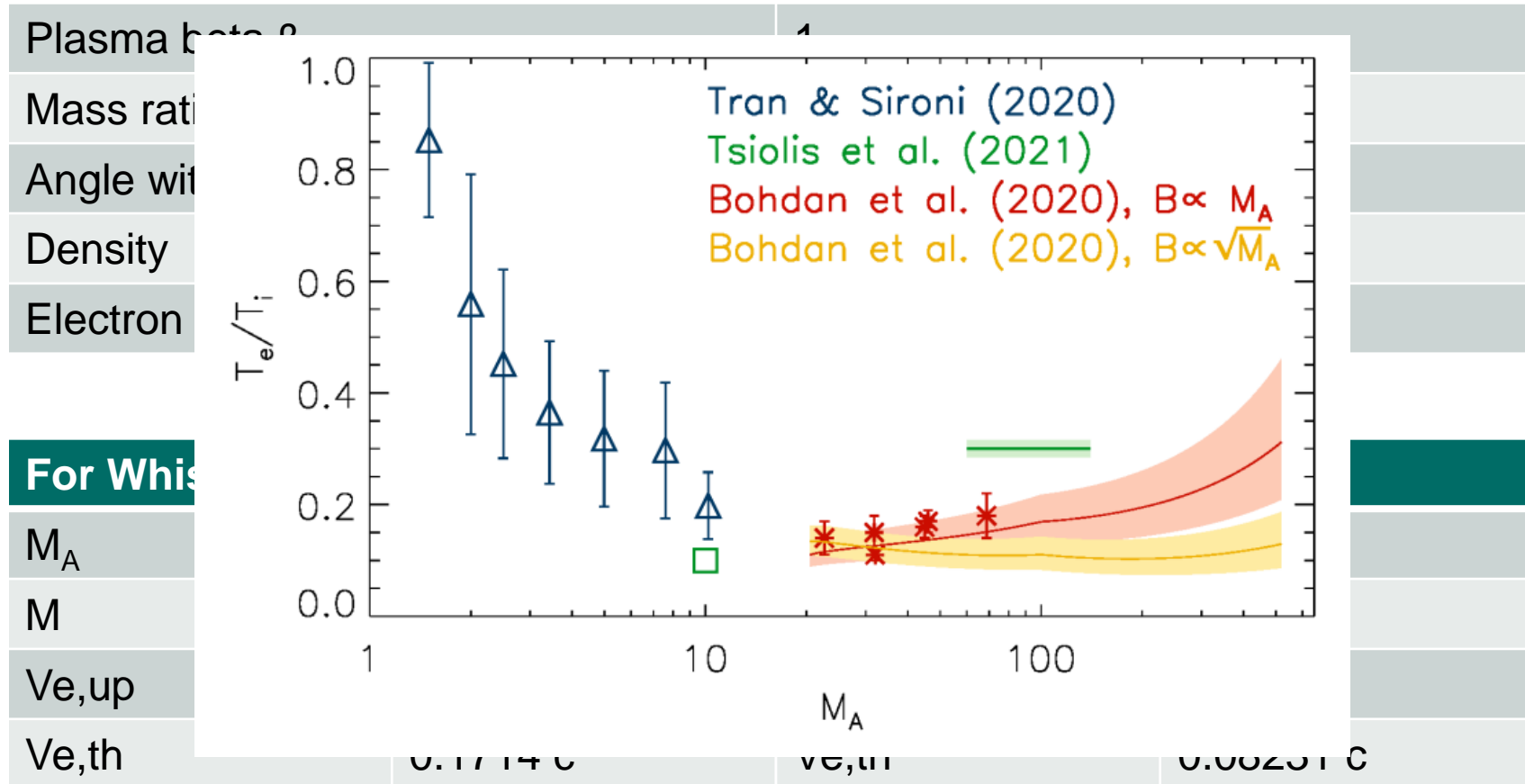
Perpendicular magnetic field.



First Simulations – Parameters



Goal : define limit cases surrounding the transition region



First Simulations – Parameters

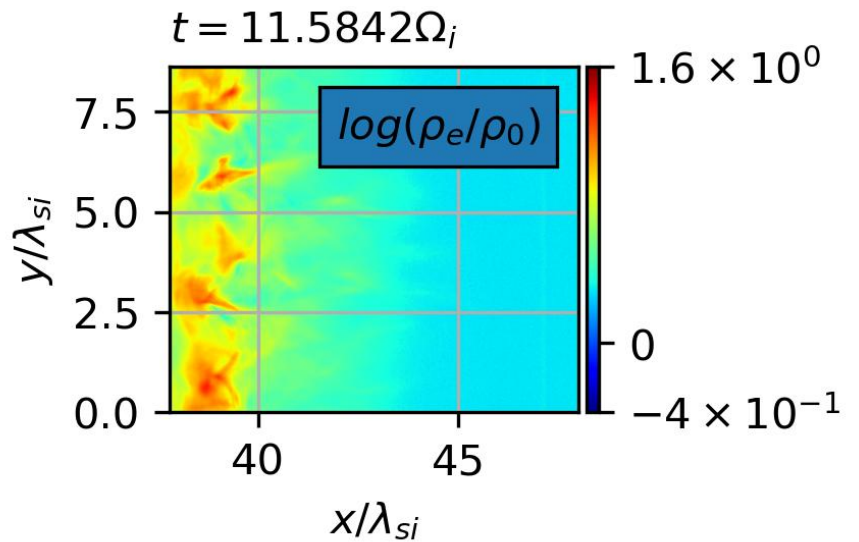
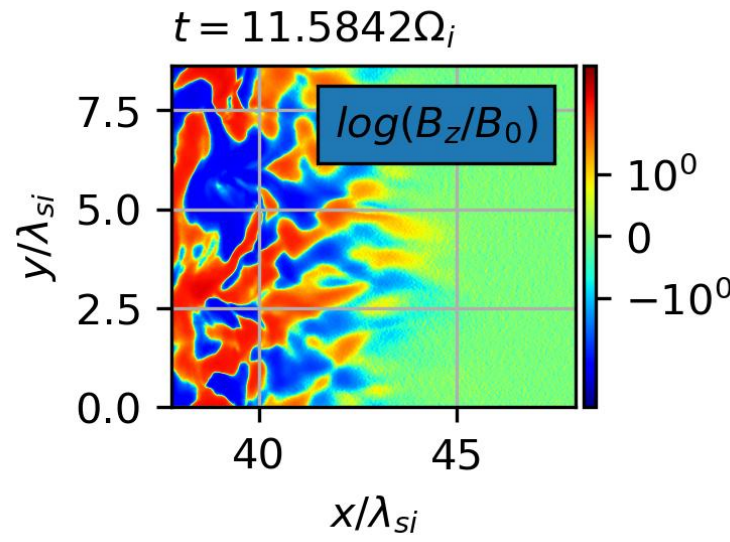
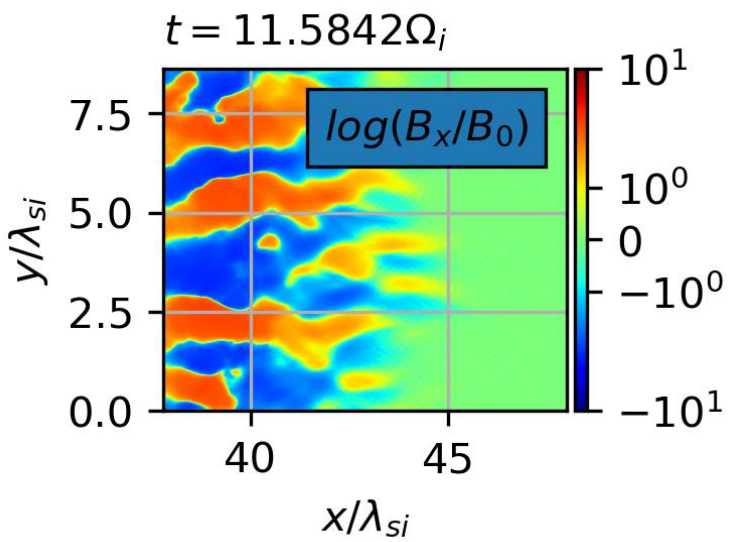
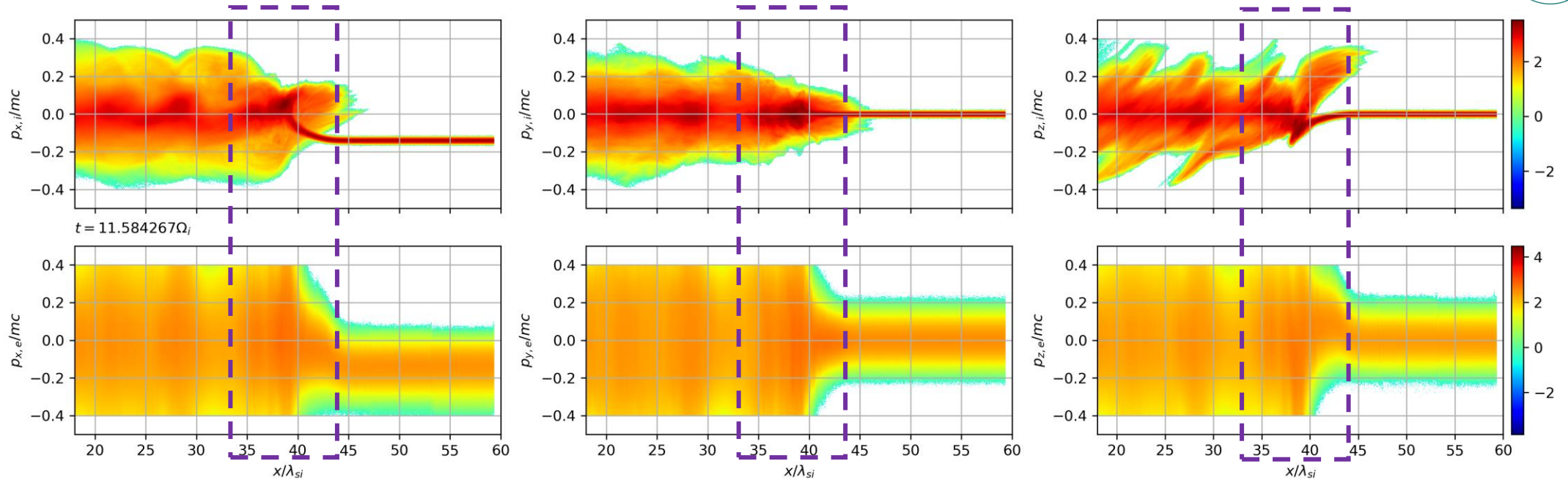


Goal : define limit cases surrounding the transition region

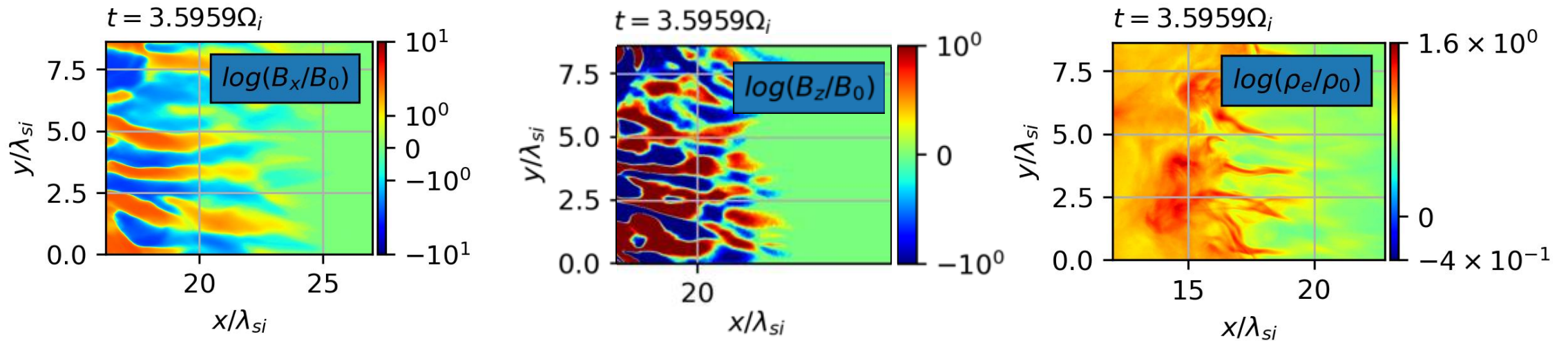
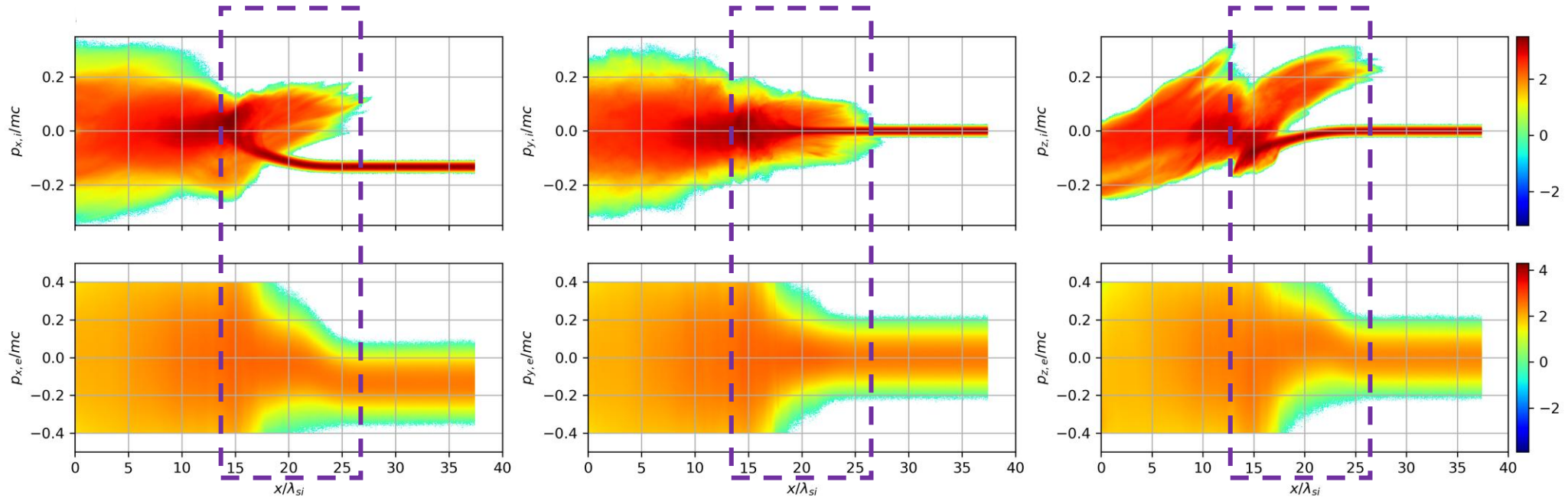
Plasma beta β_p	1
Mass ratio	100
Angle with the magnetic field	90° in x-y plane
Density	20 Particles per cell
Electron skin depth	20.0

For Whistler		For Weibel	
M_A	10	M_A	23
M_s	11	M_s	25
$V_{e,up}$	0.2694 c	$V_{e,up}$	0.1315 c
$V_{e,th}$	0.1714 c	$V_{e,th}$	0.08231 c

First Simulations – Whistler instability



First Simulations – Weibel instability

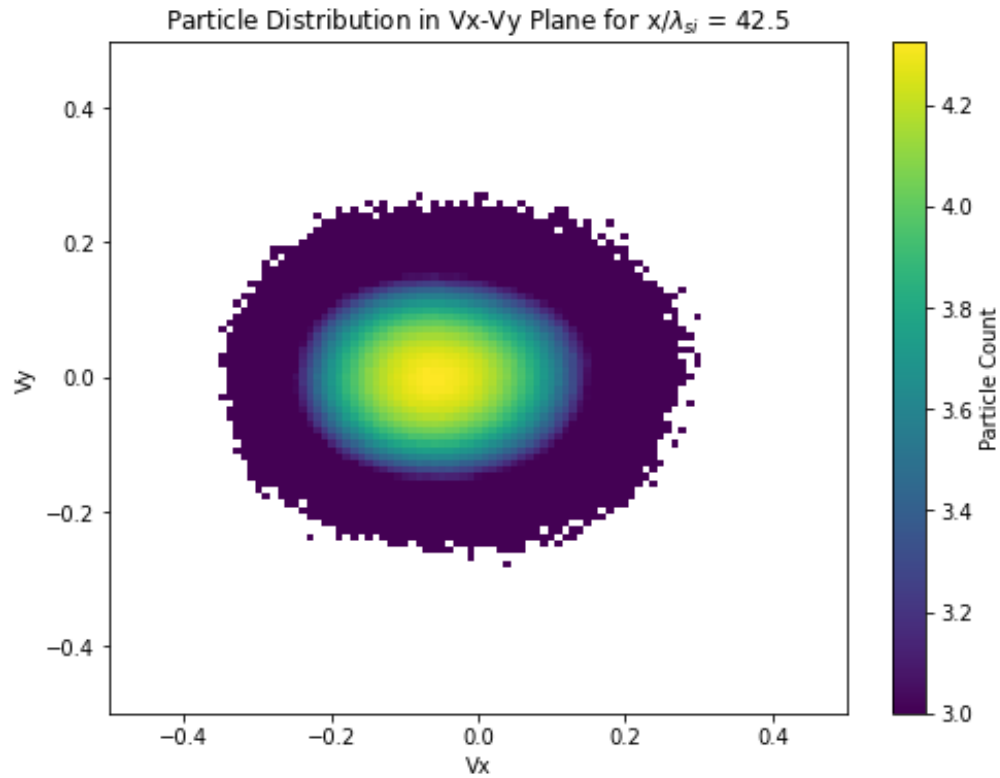


First Simulations – Comparison

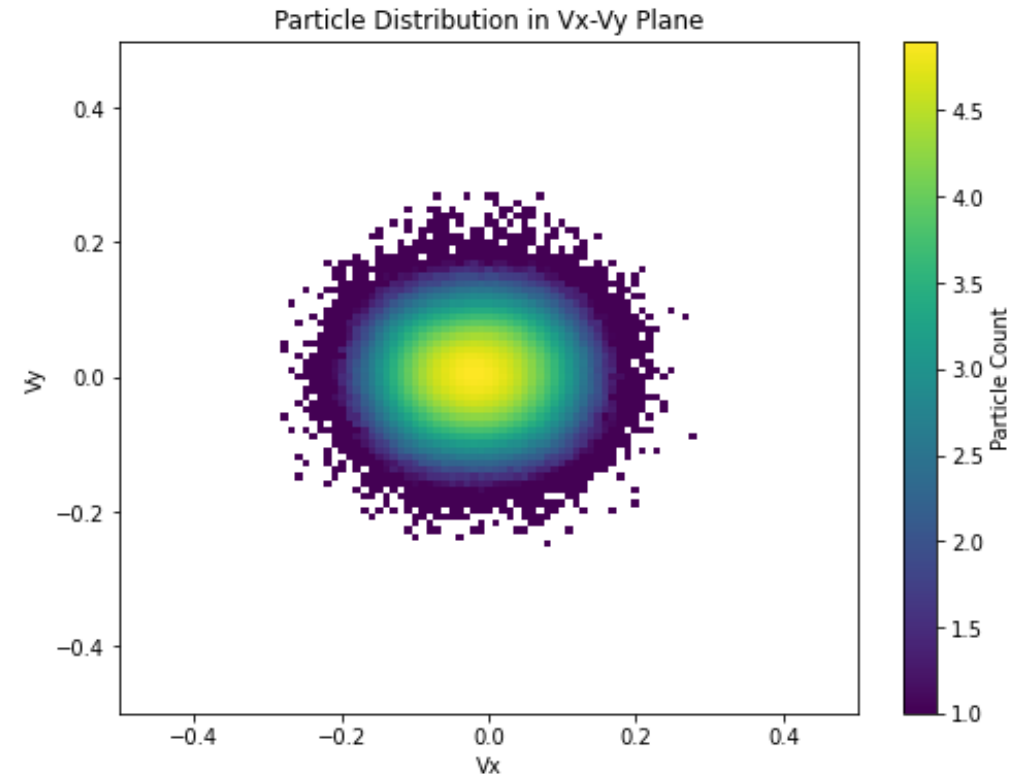
Electron and ion velocity particles distribution



Whistler



Weibel

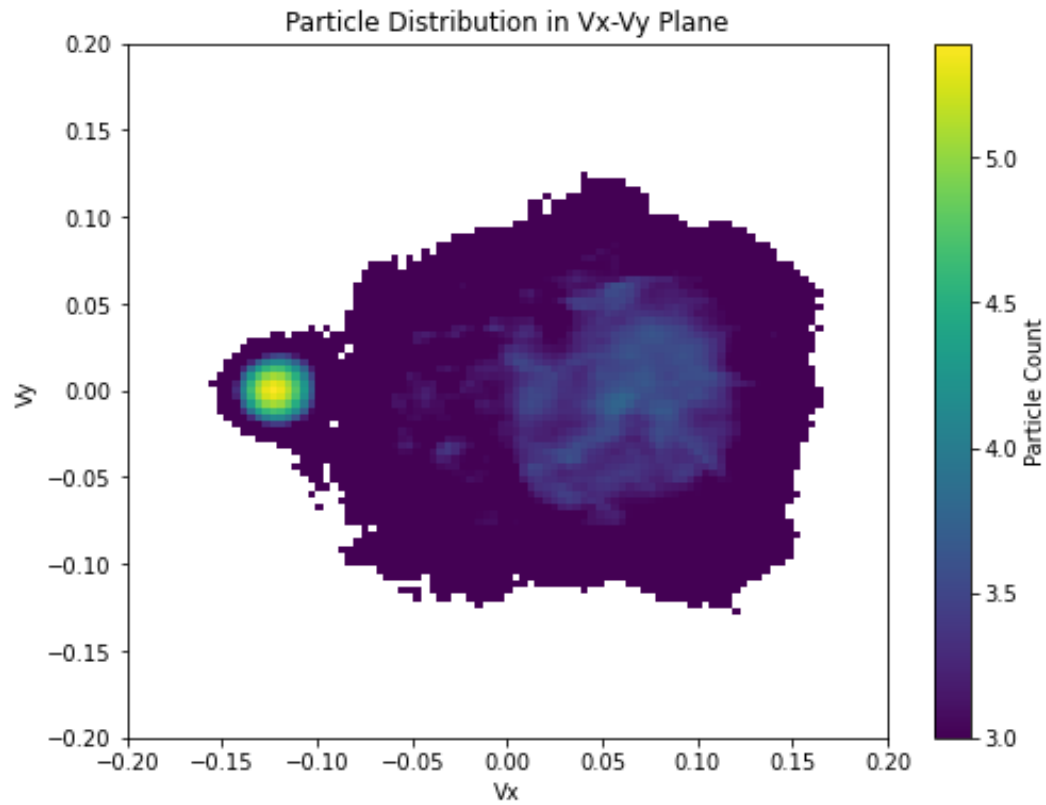


First Simulations – Comparison

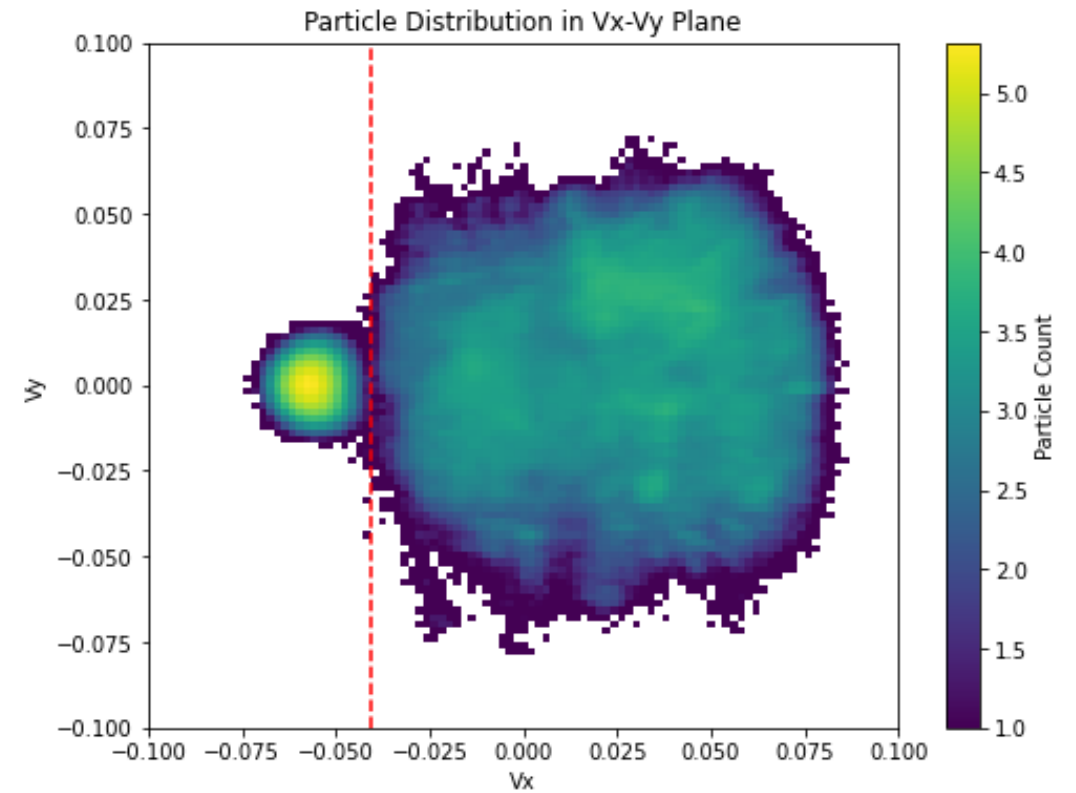
Electron and ion velocity particles distribution



Whistler



Weibel

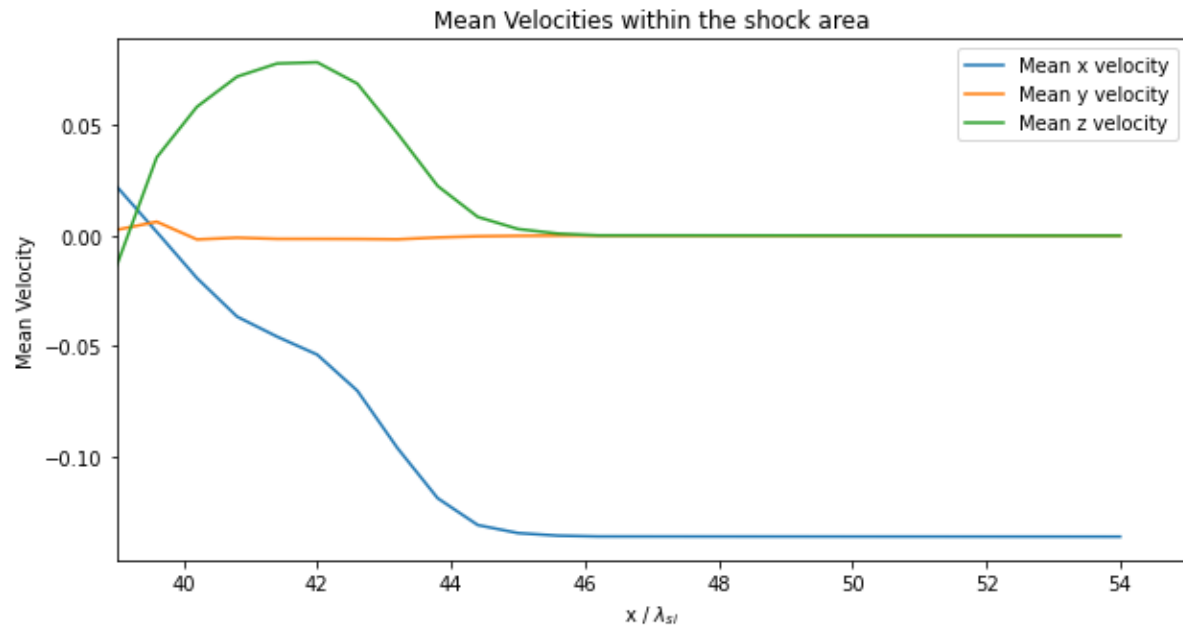


First Simulations – Comparison

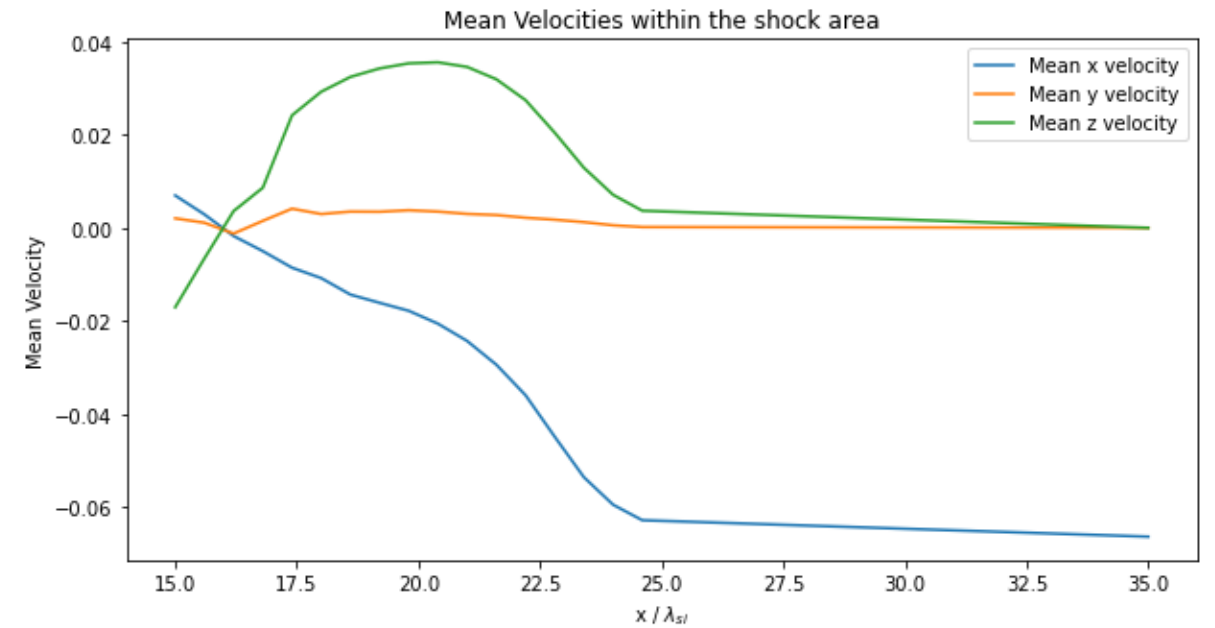
Velocities within the shock area



Whistler



Weibel



First Simulations – Comparison

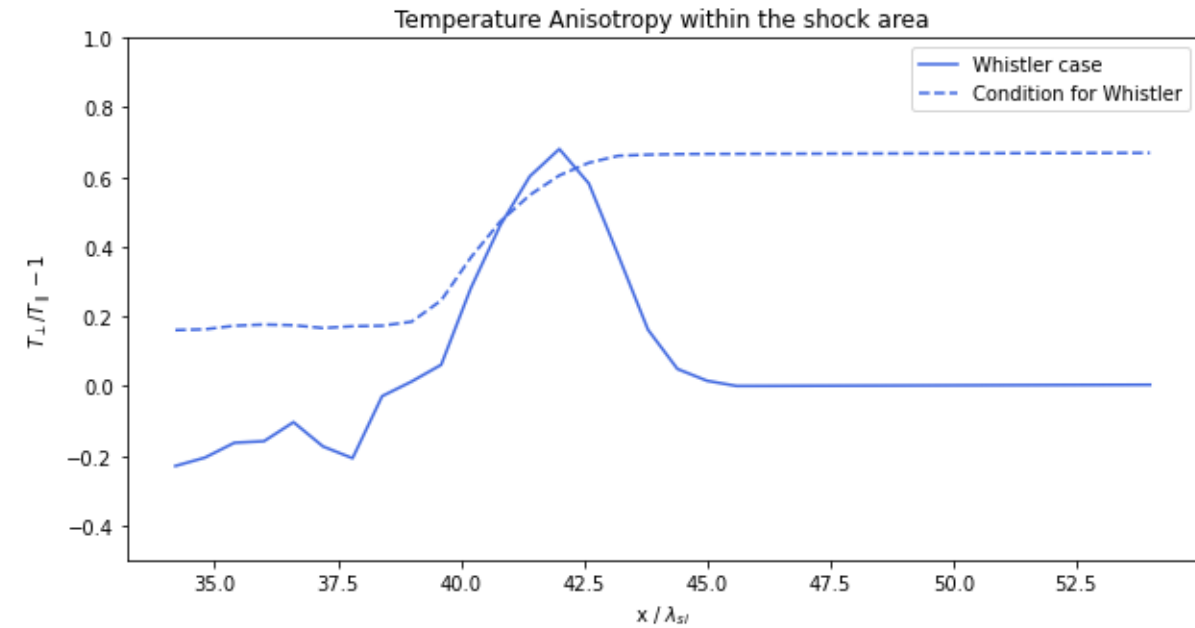
Whistler instability condition



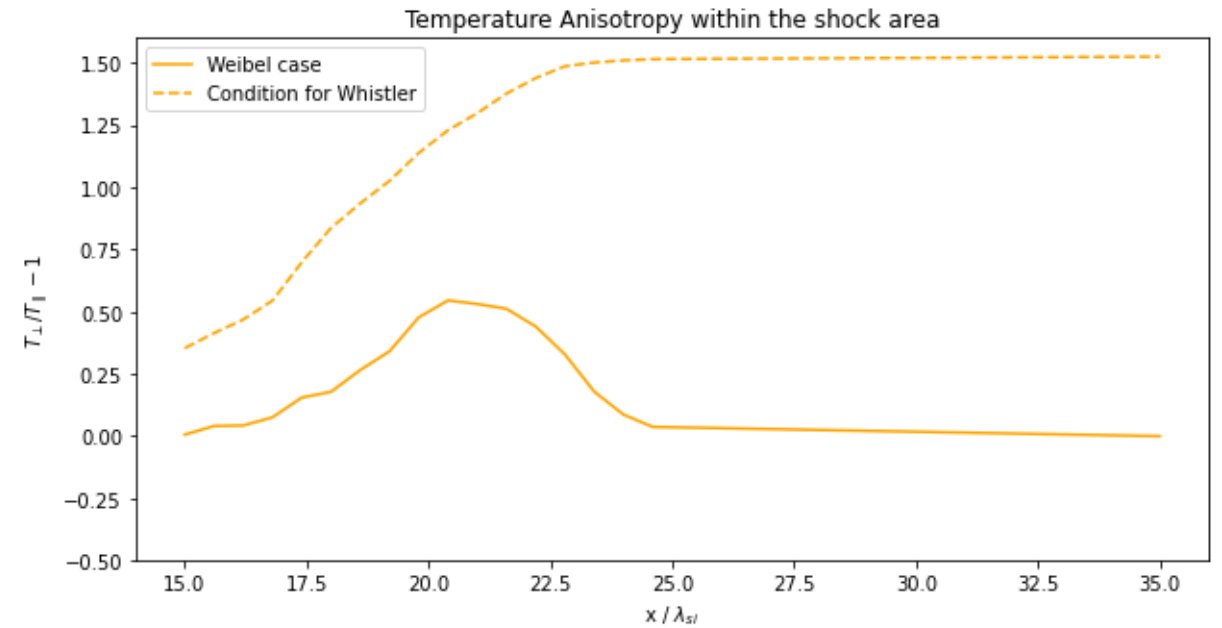
Whistler

$$\frac{T_{\perp e}}{T_{\parallel e}} - 1 \simeq \frac{0.21}{\beta_{\parallel e}^{0.6}}$$

Weibel



Threshold



Threshold

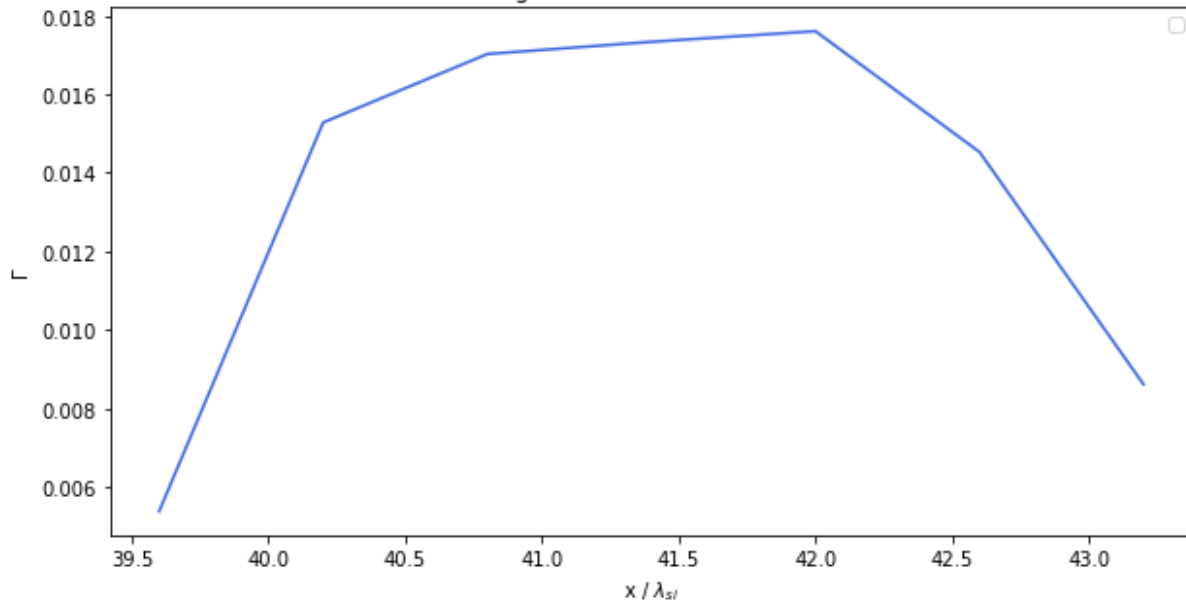
First Simulations – Comparison

Weibel growth rate



Whistler

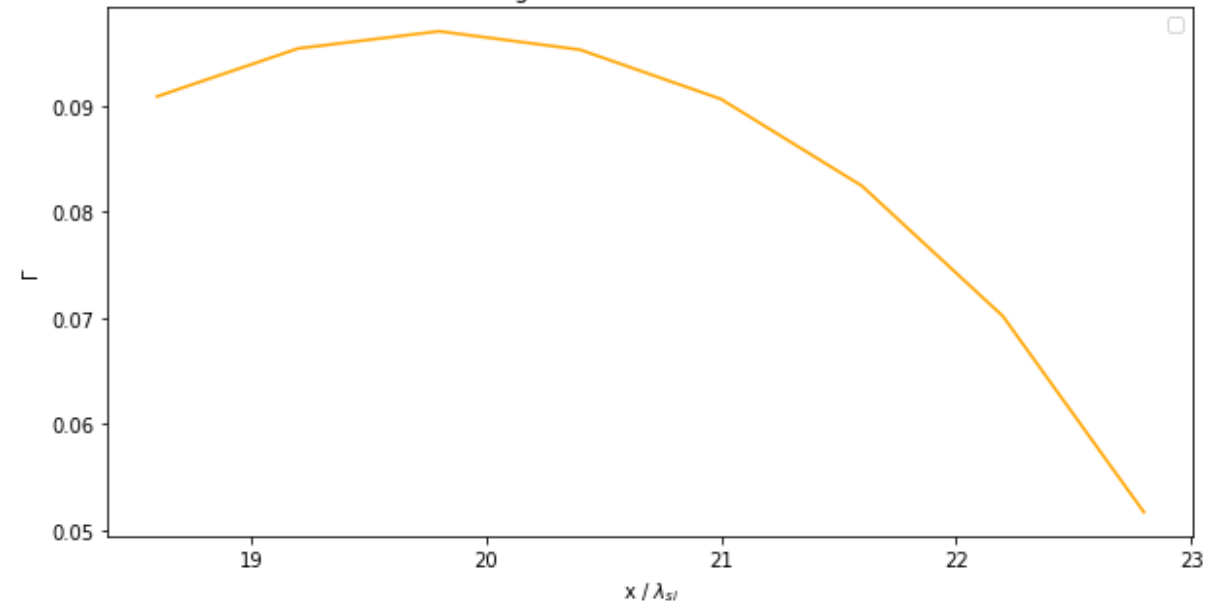
Maximum growth rate within the shock area



Max ~ 0.02

Weibel

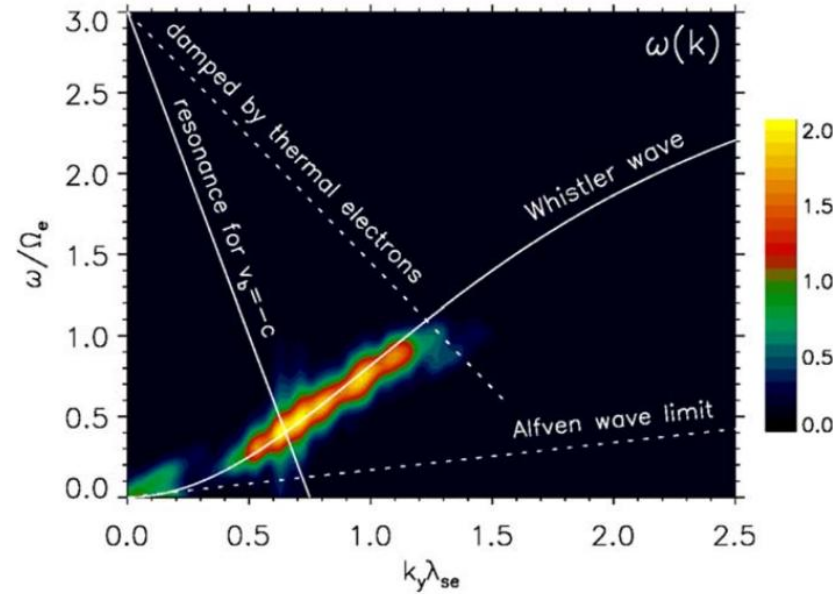
Maximum growth rate within the shock area



Max ~ 0.1

Further steps

- Fourier Spectrum



$$\omega_r(k) \sim \frac{\omega_{ce} k^2 c^2}{\omega_{pe}^2 + k^2 c^2}$$

Figure 7. Fourier spectrum of magnetic waves at, and co-moving with, the shock overshoot. The time interval is $1.63 \Omega_i^{-1} = 163 \Omega_e^{-1}$, starting from $t\Omega_i = 18$.

Plot from Kobzar et al. (2021)

→ Distinction between instabilities

- More simulations in the intermediate M_A region
 - For a set of parameters ($\beta = 1$, mass ratio = 100)

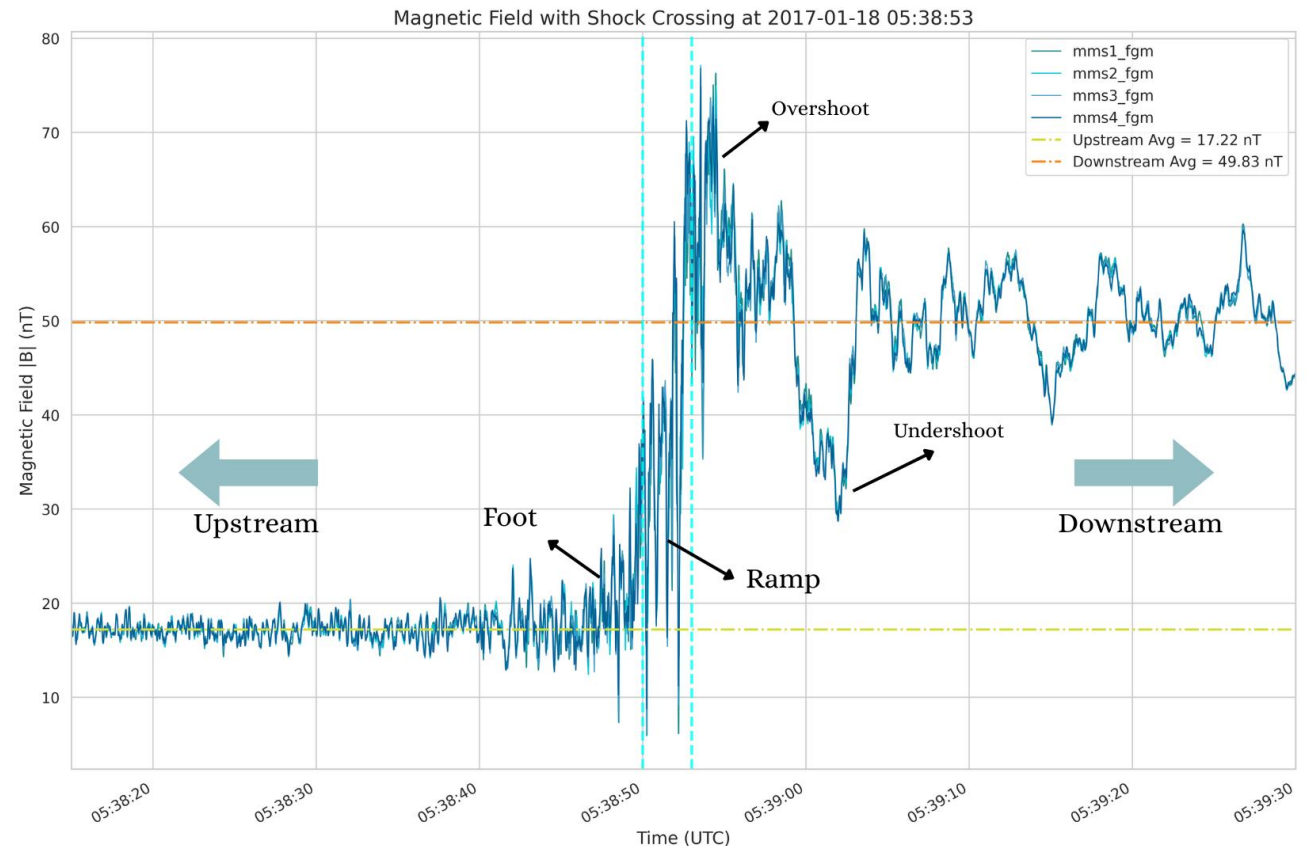
Further steps

- More simulations in the intermediate M_A region
 - Varying parameters (β , mass ratio, see Guo2017b)

- Comparison with In-situ data

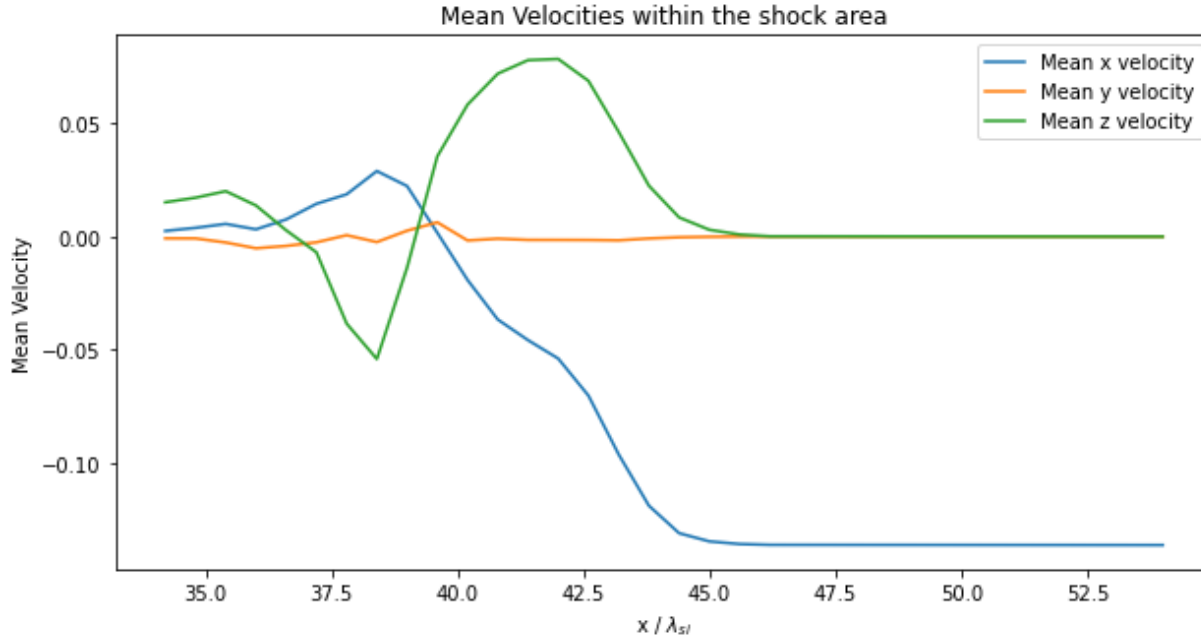
- Particle tracing

- Accelerations processes



Further steps

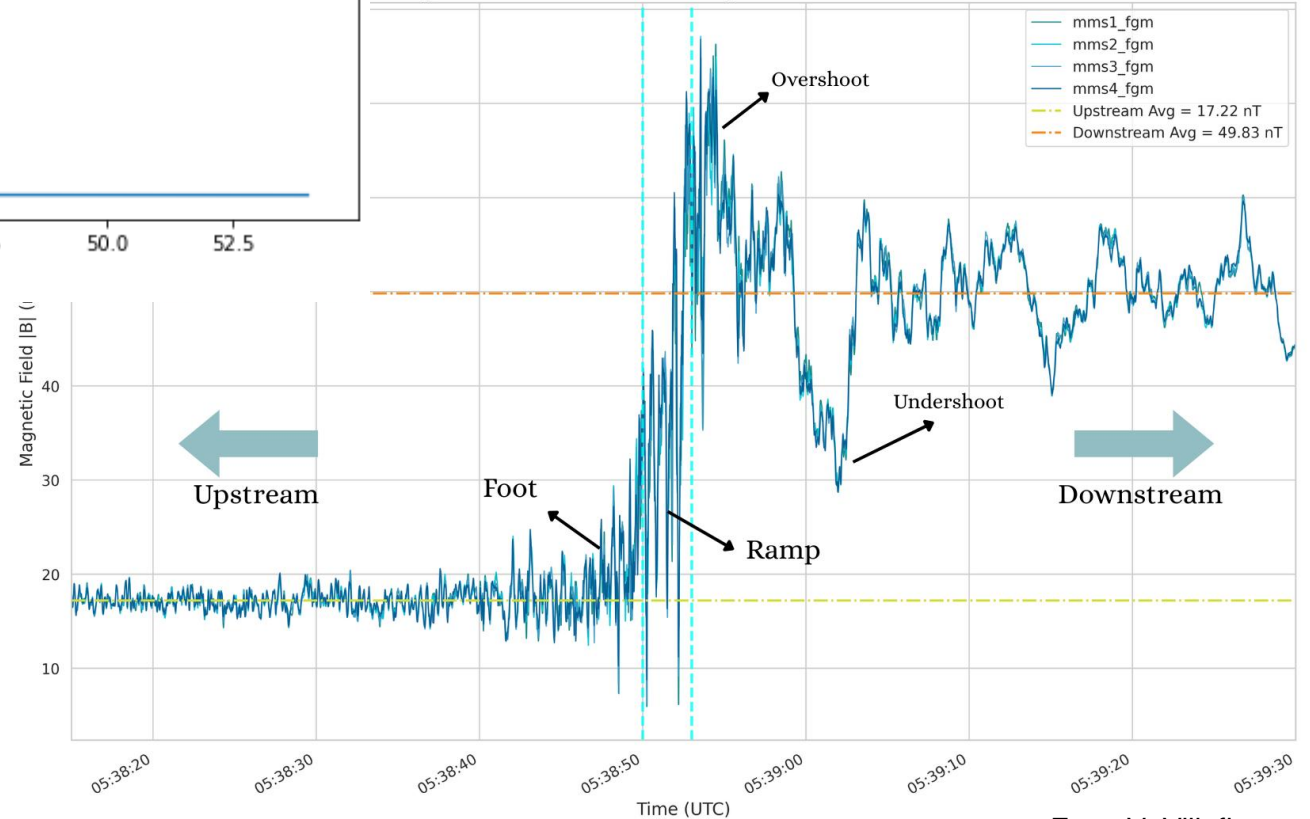
- M
- C
- Particle tracing
- Accelerations processes



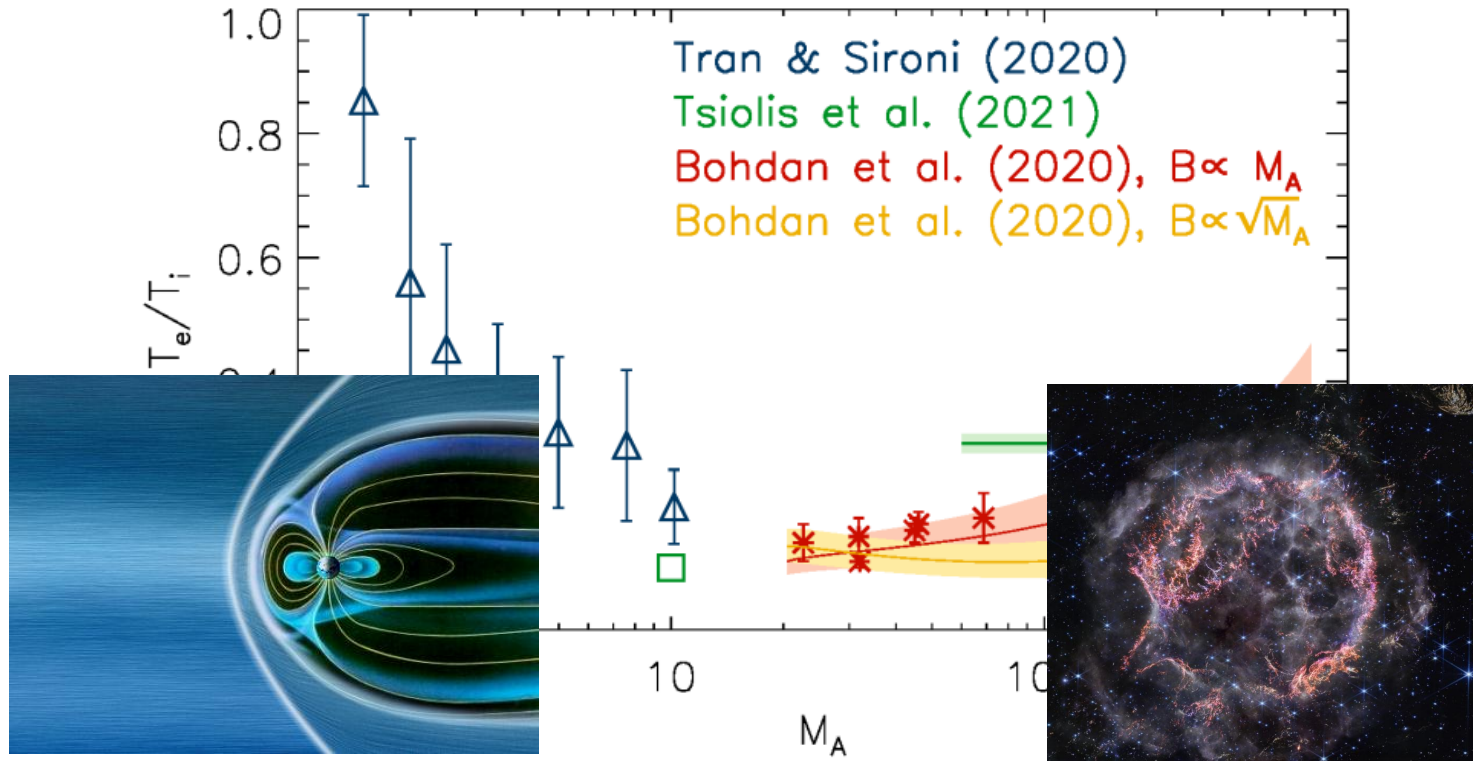
region

Guo2017b)

Magnetic Field with Shock Crossing at 2017-01-18 05:38:53



Conclusion



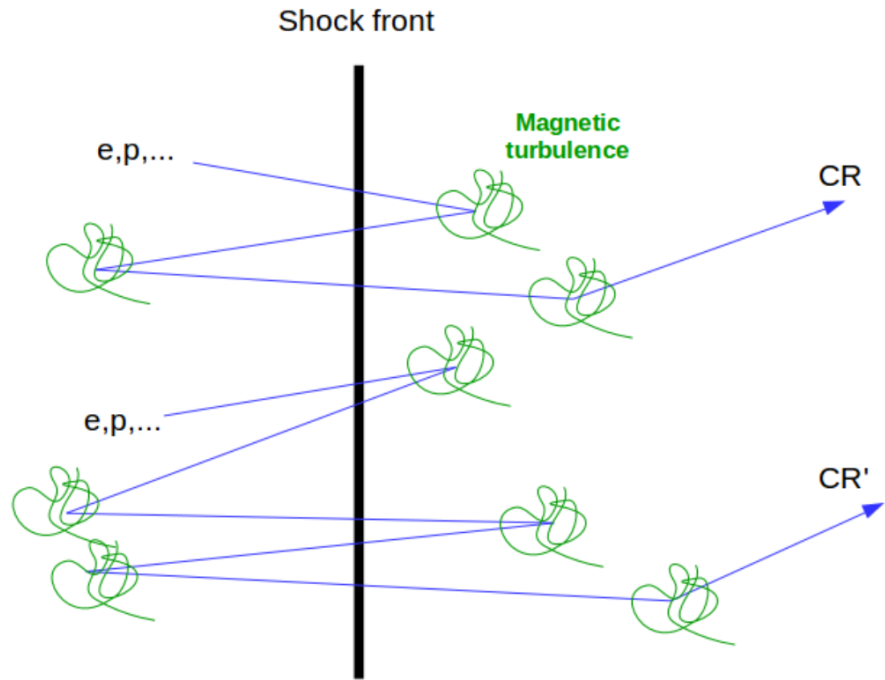
- Distinction between instabilities
- Simulations in the intermediate Mach numbers region



BACK-UP

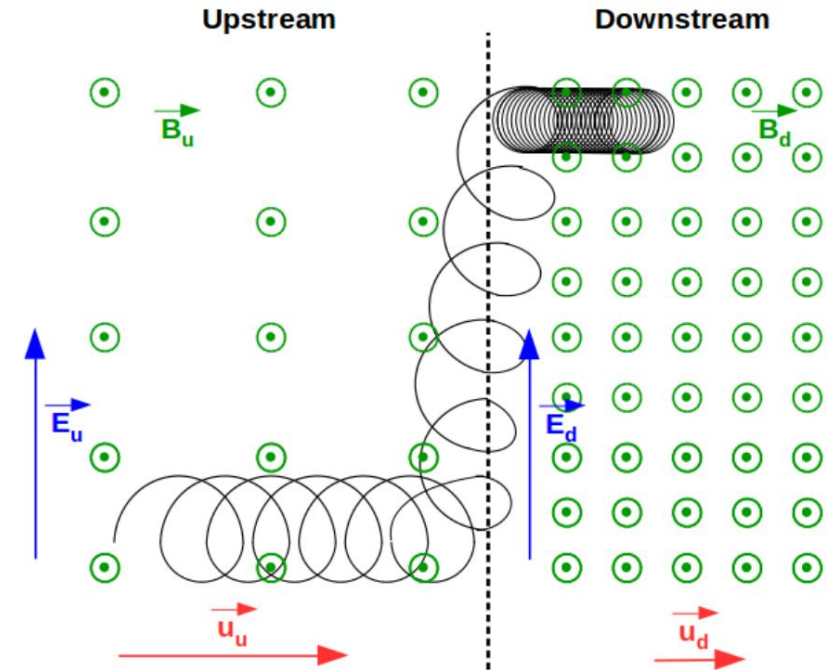
Acceleration processes

Diffusive shock acceleration (DSA)



- Multiple scatterings between upstream and downstream regions, gaining energy with each crossing
- Injection mechanism required!!

Stochastic Shock Drifting Acceleration (SSDA)



- Particles undergo random scatterings and drifts in the shock's \mathbf{B} and \mathbf{E} , resulting in their gradual acceleration.
- Within the shock's transition region.

Theoretical expectation – Whistler Instability



- Vlasov equation

$$\frac{\partial f_j}{\partial t} + \mathbf{v} \cdot \frac{\partial f_j}{\partial \mathbf{x}} + \frac{e_j}{m_j} \left(\mathbf{E} + \frac{\mathbf{v} \times \mathbf{B}}{c} \right) \cdot \frac{\partial f_j}{\partial \mathbf{v}} = 0.$$

- Small perturbations

$$f_j(\mathbf{x}, \mathbf{v}, t) = f_j^{(0)}(\mathbf{x}, \mathbf{v}) + f_j^{(1)}(\mathbf{x}, \mathbf{v}, t) + f_j^{(2)}(\mathbf{x}, \mathbf{v}, t) + \dots$$

$$\mathbf{E}(\mathbf{x}, t) = \mathbf{E}_0(\mathbf{x}) + \mathbf{E}^{(1)}(\mathbf{x}, t) + \mathbf{E}^{(2)}(\mathbf{x}, t) + \dots$$

$$\mathbf{B}(\mathbf{x}, t) = \mathbf{B}_0(\mathbf{x}) + \mathbf{B}^{(1)}(\mathbf{x}, t) + \mathbf{B}^{(2)}(\mathbf{x}, t) + \dots$$

- First velocity moment, introducing the dimensionless conductivity of the j th species

$$\Gamma_j^{(1)}(\mathbf{k}, \omega) = -\frac{ik^2 c^2}{4\pi e_j \omega} \mathbf{S}_j(\mathbf{k}, \omega) \cdot \mathbf{E}^{(1)}(\mathbf{k}, \omega)$$

$$\mathbf{S}_j(\mathbf{k}, \omega) = \frac{i}{\epsilon_0 \omega} \sigma_j(\mathbf{k}, \omega)$$

- Dispersion tensor, depending on $\mathbf{S}_j(\mathbf{k}, \omega)$

$$\mathbf{D}(\mathbf{k}, \omega) \cdot \mathbf{E}^{(1)} = 0$$

Theoretical expectation – Whistler Instability



- Linear Vlasov equation for ELM waves in magnetized plasma

$$\frac{\partial f_j^{(1)}}{\partial t} + \mathbf{v} \cdot \frac{\partial f_j^{(1)}}{\partial \mathbf{x}} + \frac{e_j}{m_j} \left(\mathbf{E}^{(1)} + \frac{\mathbf{v} \times \mathbf{B}_0}{c} \right) \cdot \frac{\partial f_j^{(1)}}{\partial \mathbf{v}} = -\frac{e_j}{m_j} \left(\mathbf{E}^{(1)}(x, t) + \frac{\mathbf{v} \times \mathbf{B}^{(1)}(\mathbf{x}, t)}{c} \right) \cdot \frac{\partial f_j^{(0)}}{\partial \mathbf{v}}$$

- First-order distribution function, using unperturbed orbit method

$$f_j^{(1)}(\mathbf{k}, v, \omega) = \frac{-e_j}{m_j} \int_{-\infty}^0 d\tau \left[\frac{\partial f_j^{(0)}}{\partial v'} + \frac{k}{\omega} \times \left(v' \times \frac{\partial f_j^{(0)}}{\partial v'} \right) \right] \cdot \mathbf{E}^{(1)}(\mathbf{k}, \omega) \exp[i b_j(\tau, \omega)]$$

where

$$b_j(\tau, \omega) = \frac{k_y v_{\perp}}{\Omega_j} [\cos(\Omega_j \tau - \phi) - \cos \phi] + (k_z v_z - \omega) \tau$$

Theoretical expectation – Whistler Instability



- $\mathbf{k} \times \mathbf{B}_0 = \mathbf{0} \longrightarrow$ ELM dispersion relation

$$\omega^2 - k^2 c^2 + k^2 c^2 \sum_j S_j^\pm(\mathbf{k}, \omega) = 0$$

- Bi-Maxwellian zeroth-order distribution function

$$f_j^{(0)}(v_z, v_\perp) = \frac{n_j}{(2\pi v_j^2)^{3/2}} \frac{T_{\parallel,j}}{T_{\perp,j}} \exp\left(-\frac{v_z^2}{2v_j^2} - \frac{v_x^2 + v_y^2}{2v_j^2} \frac{T_{\parallel,j}}{T_{\perp,j}}\right)$$

- Re-evaluation of the first-order distribution function

$$f_j^{(1)}(\mathbf{k}, \mathbf{v}, \omega) = \frac{e_j}{T_j} f_j^{(0)} \int_{-\infty}^0 d\tau \mathbf{v}' \cdot \mathbf{E}^{(1)}(\mathbf{k}, \omega) \exp[ib_j(\tau, \omega)]$$
$$- \frac{e_j}{T_j} \left(1 - \frac{T_{\parallel,j}}{T_{\perp,j}}\right) f_j^{(0)}(v_z, v_\perp)$$
$$\times \int_{-\infty}^0 d\tau \left[\mathbf{v}'_\perp \left(1 - \frac{k_z v_z}{\omega}\right) + \frac{\hat{\mathbf{z}} k_y v'_y v_z}{\omega} \right] \exp[ib_j(\tau, \omega)]$$

Theoretical expectation – Whistler Instability



- Dimensionless conductivity, for $\mathbf{k} \times \mathbf{B}_0 = \mathbf{0}$

$$S_j^\pm(\mathbf{k}, \omega) = \frac{\omega_j^2}{k^2 c^2} \left[\zeta_j^0 Z(\zeta_j^{\pm 1}) - \left(\frac{T_{\perp j}}{T_{\parallel j}} - 1 \right) \frac{Z'(\zeta_j^{\pm 1})}{2} \right]$$

- Assuming weak instability, ignoring protons and assuming electrons are nonresonant [1,2]

$$\omega_r \simeq k^2 c^2 \frac{\Omega_p}{\omega_p^2} \left[1 + \left(\frac{T_{\perp, e}}{T_{\parallel, e}} - 1 \right) \frac{\beta_e}{2} \right]$$

$$\gamma \simeq \frac{\pi}{2\omega_r} \frac{\omega_e^2}{(2\pi v_e)^{1/2}} \left[-\frac{T_{\parallel, e}}{T_{\perp, e}} \frac{\omega_r}{k_z} \pm \left(1 - \frac{T_{\parallel, e}}{T_{\perp, e}} \right) \frac{\Omega_e}{k_z} \right] \exp \left[\frac{(\omega_r \pm \Omega_e)^2}{2k_z^2 v_j^2} \right]$$

References: P. Gary 1993 [1],

Kennel & Petschek 1966 [2]

Theoretical expectation – Whistler Instability



- Necessary condition [2]:
$$\frac{T_{\perp,e}}{T_{\parallel,e}} - 1 > \frac{1}{|\Omega_e|/\omega_r - 1}$$
- By definition of the cyclotron resonance factor:
$$\frac{T_{\perp,e}}{T_{\parallel,e}} - 1 = \frac{-1}{\zeta_e^+} \left(\frac{\omega_r}{k_z v_A} \right) \left(\frac{m_e}{m_p \beta_{\parallel,e}} \right)^{1/2}$$
- Linear theory threshold [3,4]:
$$\frac{T_{\perp,e}}{T_{\parallel,e}} - 1 = \frac{S_e}{\beta_{\parallel,e}^{\alpha_e}} \quad \text{with} \quad \beta_{\parallel,e} \equiv \frac{8\pi n_e T_{\parallel,e}}{B_0^2}$$
- Numerical values [4,5]:
$$\frac{T_{\perp,e}}{T_{\parallel,e}} - 1 \simeq \frac{0.21}{\beta_{\parallel,e}^{0.6}} \quad \text{for} \quad \gamma_m = 0.001 |\Omega_e|$$

References: Kennel & Petschek 1966 [2],

P. Gary 1997 [3], P. Gary 2005 [4],

X. Guo 2017 [5].